

## Effect of functionalized multiwalled CNTs on the selective formation of calcium oxalate crystals by electrocrystallization

Andrés Vargas-Fernández, Marianela Sánchez, Felipe Díaz-Soler, Patricio Vásquez-Quitral, Mehrdad Yazdani-Pedram, and Andrónico Neira-Carrillo

*Cryst. Growth Des.*, **Just Accepted Manuscript** • DOI: 10.1021/acs.cgd.9b01067 • Publication Date (Web): 13 Dec 2019

Downloaded from [pubs.acs.org](https://pubs.acs.org) on December 23, 2019

### Just Accepted

“Just Accepted” manuscripts have been peer-reviewed and accepted for publication. They are posted online prior to technical editing, formatting for publication and author proofing. The American Chemical Society provides “Just Accepted” as a service to the research community to expedite the dissemination of scientific material as soon as possible after acceptance. “Just Accepted” manuscripts appear in full in PDF format accompanied by an HTML abstract. “Just Accepted” manuscripts have been fully peer reviewed, but should not be considered the official version of record. They are citable by the Digital Object Identifier (DOI®). “Just Accepted” is an optional service offered to authors. Therefore, the “Just Accepted” Web site may not include all articles that will be published in the journal. After a manuscript is technically edited and formatted, it will be removed from the “Just Accepted” Web site and published as an ASAP article. Note that technical editing may introduce minor changes to the manuscript text and/or graphics which could affect content, and all legal disclaimers and ethical guidelines that apply to the journal pertain. ACS cannot be held responsible for errors or consequences arising from the use of information contained in these “Just Accepted” manuscripts.

# Effect of functionalized multiwalled CNTs on the selective formation of calcium oxalate crystals by electrocrystallization

*Andrés Vargas-Fernández,<sup>†</sup> Marianela Sánchez,<sup>†</sup> Felipe Díaz-Soler,<sup>†</sup> Patricio Vásquez-Quitral,<sup>‡</sup> Mehrdad Yazdani-Pedram,<sup>§</sup> and Andrónico Neira-Carrillo<sup>\*†</sup>*

<sup>†</sup>Department of Biological and Animal Science, University of Chile. Santa Rosa 11735. La Pintana, Santiago, Chile.

<sup>‡</sup> Department of Organic and Physical Chemistry, University of Chile. S. Livingstone 1007. Independencia, Santiago, Chile.

<sup>§</sup> Instituto de Ciencias Químicas Aplicadas, Facultad de Ingeniería, Universidad Autónoma de Chile, San Miguel, Santiago 8900000, Chile.

**ABSTRACT:** The electrocrystallization (EC) of calcium oxalate (CaOx) crystals in the presence of multiwalled CNTs (MWCNT) functionalized with itaconic acid (IA) and the monoester derivatives mono-methylitaconate (MMI) or mono-octadecylitaconate (MODI), which were used as new IA-ester templates supported on indium tin oxide (ITO) glass substrate as working electrode, were performed by applying a 9-mA current at 37 °C and 60 °C for 5 min. Under the above EC reaction conditions, a broad variety of CaOx morphologies and crystal forms was

1  
2  
3 found. The morphology control and coexistence of CaOx monohydrate (COM) and CaOx  
4 dihydrate (COD) was achieved through *in vitro* EC according to XRD spectra. We found that all  
5 the functionalized MWCNTs were more efficient inhibitors of CaOx crystallization than the  
6 typical citrate model, where MWCNT-IA was the most effective stabilizing template of COM  
7 crystals due to the fact that carboxylic acid groups of IA moieties in MWCNT-IA would be  
8 better Ca<sup>2+</sup> ions-binding sites than IA ester groups.  
9

10  
11  
12 **KEYWORDS:** Multiwalled carbon nanotube (MWCNT), itaconic acid (IA), calcium oxalate,  
13 electrocrystallization, CaOx monohydrate (COM), CaOx dihydrate (COD)  
14  
15  
16  
17

## 18 19 20 21 22 23 24 25 **1. INTRODUCTION**

26  
27  
28 Biom mineralization is the formation of biogenic minerals with biological origins, such as  
29 vertebrate bone and teeth, invertebrate shells and exoskeletons and even small particles secreted  
30 by plants and bacteria.<sup>1,2</sup> Kidney stones (KS) are the result of pathological biom mineralization  
31 caused by the uncontrolled nucleation of CaOx.<sup>3</sup> KS can occur in different animal species; CaOx  
32 is one of the most copious minerals present in plants and is the most abundant mineral found in  
33 urinary calculi produced by mammals, including humans.<sup>4,5</sup>  
34  
35  
36  
37  
38  
39  
40  
41

42 CaOx is known to have three structural main forms: the monoclinic monohydrate (COM,  
43 whewellite), tetragonal dihydrate (COD, weddellite) and triclinic trihydrate (COT).<sup>6,7</sup> These  
44 hydrates differ in their size, morphology and stability, and COM is the most stable.<sup>8</sup> COD and  
45 COM are often found in urinary calculi, inducing crystal agglomeration, and COM strongly  
46 adheres to the epithelium of renal cells.<sup>9</sup> Instead, COD avoids the formation of KS by adsorbing  
47 urinary molecules, thus decreasing urolithiasis risk.<sup>10</sup> Therefore, studying the nucleation process  
48  
49  
50  
51  
52  
53  
54  
55  
56  
57  
58  
59  
60

1  
2  
3 of KS has led to a renewed interest in evaluating the effects exerted by different additives on  
4 CaOx crystallization. The controlled crystallization of CaOx has been performed in organic  
5 media using synthetic molecules and natural biomolecules as inhibitors.<sup>11,12</sup>  
6  
7

8  
9  
10 A method rarely used to evaluate the role of additives on the mineralization of oxides and  
11 inorganic materials is the electrocrystallization (EC) technique known as electrodeposition  
12 method, in which that electrochemical deposition is a general method of fabrication of oxide or  
13 mineral coating.<sup>13-15</sup> This method can be used to direct oriented crystallization or selectively  
14 control the crystal morphology. EC seems to be an appropriate method for understanding the  
15 different aspects of biomineralization due to there are few instances of the study of  
16 polymorphism of inorganic mineral by electrochemistry, parameters such as nucleation and  
17 crystal growth could be addressed, and could even be utilized to study the stabilization of  
18 metastable forms.<sup>16</sup> Joseph and Kamath found that CaOx nucleation was affected by changing  
19 the pH (9 and 11), current density (3 mA and 6 mA) and temperature (23 °C and 65 °C). The  
20 research to date has established that the morphology, size and type of CaOx crystals are  
21 controlled by not only the crystallization method but also the variation of experimental  
22 parameters such as the concentration, molar ratio of the reactants, pH, time and effect of  
23 temperature has been studied in the *in vitro* CaOx crystallization.<sup>17</sup>  
24  
25  
26  
27  
28  
29  
30  
31  
32  
33  
34  
35  
36  
37  
38  
39  
40  
41  
42  
43

44 On the other hand, multiwalled CNTs (MWCNTs) have been used for diverse high-tech  
45 applications, such as catalysis, hydrogen storage, nanoelectronics, optics, solar cells, medicine,  
46 among other application areas. Carbon-based nanomaterials and CNTs have been extensively  
47 investigated as sensitive rheological additives for a range of nanocomposites. In spite of its long  
48 success in these diverse applications, MWCNTs have been sparsely used as template for the  
49 mineralization of calcium-salts, which is probably due to their hydrophobic character and  
50  
51  
52  
53  
54  
55  
56  
57  
58  
59  
60

1  
2  
3 chemical inertness.<sup>18-20</sup> However, combination of carbon-based nanomaterials with calcium-salts  
4  
5 such as calcium carbonate, hydroxyapatite, carbides, silica - titania oxide materials, among  
6  
7 others have been utilized, since the combination of these materials offers great functional  
8  
9 advantages over conventional materials currently employed in construction.<sup>21</sup> Moreover, carbon  
10  
11 allotropes such as fullerenes and single walled CNTs also influence the synthesis of CaCO<sub>3</sub>  
12  
13 materials resulting in amorphous phases with unique and interesting morphologies.<sup>22</sup> In case of  
14  
15 CaOx, abundant natural urinary macromolecules and plant extract have been also tested as  
16  
17 modifier acting as inhibitor of COM crystallization kinetics *in vitro*.<sup>23,24</sup> The precise interactions  
18  
19 of these macromolecules with COM are yet unknown. The type of CNTs functionalization *e.g.*  
20  
21 covalent and non-covalent reported by Tasis *et al.* demonstrated that the interface between the  
22  
23 carbon nanomaterial and the growth medium of the inorganic mineral are extremely important as  
24  
25 well as tubular structure of CNTs providing more favorable morphology for inorganic materials  
26  
27 as reported for hydroxyapatite when compared to other carbon-base materials.<sup>25,26</sup> Therefore, the  
28  
29 grafting of hydrophilic molecules such as IA to the highly hydrophobic CNT allows obtaining  
30  
31 new template with potential Ca<sup>2+</sup> ions-binding capability. The strategy used here may contribute  
32  
33 to broaden the use of functionalized MWCNTs with different hydrophilic molecules allowing to  
34  
35 control selective *in vitro* crystallization of variety of inorganic minerals. With this background in  
36  
37 mind, we believe that the selective chemical modification of MWCNTs may allow the control of  
38  
39 the nucleation and growth of inorganic materials to achieve nanostructures with defined sizes,  
40  
41 shapes, and compositions.<sup>27,28</sup> On the other hand, the kinetic aspects of *in vitro* CaOx  
42  
43 crystallization using active modifier molecules at different concentrations and temperatures is the  
44  
45 basis for *in vivo* assays and is the first approach for the urolithiasis medication. Indeed, for *in*  
46  
47 *vivo* delivery of drugs using implantable peristaltic mini pumps allows to foresee the classic  
48  
49  
50  
51  
52  
53  
54  
55  
56  
57  
58  
59  
60

1  
2  
3 problems such as of solubility, concentration, control of small-volume of release, dose-response  
4  
5 behavior to achieve a greater effect of pathological crystal inhibition using urolithiasis drugs.  
6  
7

8  
9 The aim of this paper is to report the *in vitro* EC of CaOx in the presence of MWCNTs modified  
10  
11 with itaconic acid (IA) and monoester derivatives, namely, monomethyl itaconate (MMI) or  
12  
13 monoctadecyl itaconate (MODI), and supported on an indium tin oxide (ITO) glass substrate,  
14  
15 which is used as the working electrode by applying a 9-mA current for 5 min at 37 °C and 60 °C.  
16  
17 Chrono-potentiometric measurements of CaOx were successfully performed with all the  
18  
19 functionalized MWCNTs, and these results were compared with citrate. These conditions were  
20  
21 selected by first considering the potential value, where the reduction of molecular oxygen (O<sub>2</sub>  
22  
23 saturation) reached its highest activity and secondly this optimized potential was applied in order  
24  
25 to assure a stable electrochemical response, controlled size and morphology of CaOx crystals.  
26  
27  
28

29  
30 The experimental setup and procedure used for the measurement of the EC of CaOx are shown in  
31  
32 Figure 1.  
33  
34

### 35 36 **Figure 1.**

## 37 38 39 **2. EXPERIMENTAL SECTION**

### 40 41 42 **2.1 Materials and Chemicals.**

43  
44 A detailed description of the materials, chemical reagents, oxidation and functionalization of  
45  
46 the MWCNTs is available in the Supporting Information.  
47  
48

### 49 50 **2.2. Electrocrystallization of CaOx.**

51  
52 The *in vitro* EC of CaOx was performed for 5 min on ITO substrates heated to either 37 °C or  
53  
54 60 °C, and a 9-mA current was applied in the absence or presence 0.03 mg/mL MWCNT in an  
55  
56 electrochemical cell (ECC). The negative and positive controls were prepared by performing the  
57  
58  
59

1  
2  
3 EC of CaOx in the absence of the additive and in the presence of sodium citrate, respectively.  
4  
5 Briefly, for the EC of CaOx assays, 50 mM calcium nitrate tetrahydrate solutions and 75 mM  
6  
7 ethylenediaminetetraacetic acid were mixed and sonicated for 5 min, and the pH was adjusted to  
8  
9 10.5 by adding 1 M NaOH dropwise. This solution was mixed with a 50 mM sodium oxalate  
10  
11 solution containing 0.75 mg of each MWCNTs and sonicated for 5 min. Then, 25 mL of the  
12  
13 resulting electrolytic solution was poured into the glass ECC. To test the effect of all MWCNTs  
14  
15 as templates on the CaOx ECC a chrono-potentiometry was performed. The applied potential  
16  
17 range was +/- 10 V with a sample interval of 2 sec with the applied current of 9-mA. The ECC  
18  
19 measurements were conducted using ITO substrates as the working electrodes (WE), a coiled  
20  
21 platinum (Pt) wire as the auxiliary electrode (AE) and a silver chloride electrode (Ag/AgCl) as  
22  
23 the reference electrode (RE). The washing and sonication protocols are provided in the  
24  
25 Supporting Information.  
26  
27  
28  
29

### 30 31 **2.3 Characterization.** 32

33  
34 The surface morphology and microanalysis of the resultant CaOx crystals were observed by  
35  
36 scanning electron microscopy (SEM) coupled with energy dispersive X-ray (EDX) analysis; the  
37  
38 elemental analysis was performed with computer-controlled software. The SEM-EDX analysis  
39  
40 was carried out by using a JEOL JSM-IT300LV microscope (JEOL USA Inc., USA) and an  
41  
42 Aztec EDX system (Oxford Instruments, Abingdon, UK). A Hitachi TM3000 tabletop  
43  
44 microscope (Hitachi High Tech) coupled with Quantax 70 EDX spectrometer (Bruker, Germany)  
45  
46 and equipped with a high-sensitivity BSE semiconductor detector was also used. The FTIR  
47  
48 analyses of the pristine, oxidized and functionalized MWCNTs were performed by Fourier  
49  
50 transform infrared spectroscopy/Attenuated total reflection (FTIR-ATR) using an Interspectrum  
51  
52 Interspec p/n 200-X instrument. TEM images of MWCNTs used as templates were obtained with  
53  
54  
55  
56  
57  
58  
59  
60

1  
2  
3 a Philips Tecnai 12 Bio Twin 120 K transmission electron microscope. Chrono-potentiometry  
4 was carried out during the CaOx EC using a Potentiostat/Galvanostat BASi Epsilon (USA)  
5 instrument. Powder X-ray diffraction (PXRD) of the CaOx crystals was performed by using a  
6  
7 Siemens D-5000X X-ray diffractometer with Cu-K $\alpha$  radiation (graphite monochromator) and an  
8 ENRAF Nonius FR 590 X-ray generator. The crystal structure of CaOx was determined by using  
9  
10 Cu-K $\alpha$  radiation (40 kV), step sizes of 0.2 $^\circ$ , and the geometric Bragg-Brentano ( $\theta$ - $\theta$ ) scanning  
11  
12 mode with an angle ( $2\theta$ ) in the range of 5-70 $^\circ$ . The DiffracPlus program was used as the data  
13  
14 control software.  
15  
16  
17  
18  
19  
20  
21  
22  
23  
24  
25

### 26 **3. RESULTS AND DISCUSSION**

27  
28  
29  
30  
31  
32 To study the effect of MWCNTs functionalized with IA and IA derivatives on CaOx  
33 crystallization, a preliminary set of CaOx crystals prepared by EC were examined using two  
34 experimental setups, which consisted of an open or a closed EC system in the absence of  
35  
36 MWCNTs template and with a current applied from 1- 24 mA for 5 min at 23  $^\circ$ C, 37  $^\circ$ C and 60  
37  
38  $^\circ$ C (Table 1).  
39  
40  
41  
42  
43  
44

45 **Table 1.**

46  
47  
48 In addition, the chrono-potentiometric measurements were obtained during the EC of CaOx  
49 (Figure S1), and an optical and electron microscopy analyses of the CaOx crystals in both the EC  
50 systems, where a 1 - 24 mA current was applied for 5 min at 23  $^\circ$ C, 37  $^\circ$ C and 60  $^\circ$ C, were  
51  
52 carried out (Figure S2). The potentiometric response in the ECC during the CaOx EC was larger  
53  
54  
55  
56  
57  
58  
59  
60



1  
2  
3 and more stable in the closed system, and the same electrochemical behavior was observed at all  
4 the abovementioned temperatures. Therefore, after analyzing the results obtained at different  
5 temperatures and applied currents as well as the optical and electron microscopy and chrono-  
6 potentiometry results, we focused this study to evaluate the effect of the morphology and  
7 polymorphism modulation capability of the pristine and functionalized MWCNTs on the *in vitro*  
8 EC of CaOx by applying a 9-mA current at 37 °C and 60 °C. Moreover, the elemental chemical  
9 composition of the CaOx crystals obtained in the open and closed EC systems was confirmed by  
10 EDX (Table S1). Figure 2 shows the chrono-potentiometric measurements obtained during the  
11 EC of CaOx by using both the open and closed EC systems via applying a 9-mA current for 5  
12 min at 37 °C and 60 °C. The same electrochemical behavior was observed for both of the  
13 systems at 37 °C and 60 °C. Figure 2A shows that the potentiometric response curves for the  
14 open system begins at a lower potential value of 1.73 V with respect to the closed system, which  
15 starts at 1.84 V, and the final potential values were 2.37 V and 2.09 V at 37 °C and 60 °C,  
16 respectively. We found that the starting and final potentiometric response curves recorded during  
17 the open EC system were lower than those recorded for the closed system. Figure 2 B shows the  
18 potentiometric response curves realized in the closed EC system, where the initial potential  
19 values started at 2.06 V and 2.62 V, and the final potential values were 2.35 V and 2.94 V at 37  
20 °C and 60 °C, respectively. Comparing the two experimental results, it can be seen that the  
21 closed EC system of CaOx was more stable and exhibited an independent potentiometric  
22 response at 37 °C and 60 °C.  
23  
24  
25  
26  
27  
28  
29  
30  
31  
32  
33  
34  
35  
36  
37  
38  
39  
40  
41  
42  
43  
44  
45  
46  
47  
48  
49

### 50 **Figure 2.**

51  
52 The experimental procedures of the *in vitro* EC of CaOx and the physicochemical  
53 characterization of the MWCNTs can be found in the Supporting Information. The Fourier  
54  
55  
56  
57  
58  
59  
60

1  
2  
3 transform infrared (FTIR) spectra of pristine MWCNT, MWCNT-IA, MWCNT-MMI and  
4  
5 MWCNT-MODI are shown in Figure S3. The presence of O-H groups of adsorbed water  
6  
7 in pristine MWCNT, the stretching vibrations of the vinyl C=C bonds and carboxylic groups of  
8  
9 IA in MWCNT-IA, as well as absorption bands corresponding to C=C vinyl double bond, C=O  
10  
11 of carboxyl and ester groups of MMI in MWCNT-MMI and MODI in MWCNT-MODI were  
12  
13 confirmed by FTIR spectroscopy. All absorption bands designation of MWCNTs functionalized  
14  
15 with IA, MMI and MODI were discussed in detail in the section 1.4 of the SI. The morphology  
16  
17 of the MWCNTs was analyzed by transmission electron microscopy (TEM). The TEM images of  
18  
19 pristine MWCNT and all functionalized MWCNT-IA, MWCNT-MMI and MWCNT-MODI  
20  
21 templates are shown in Figure S4 in the Supporting Information. Similar TEM images of  
22  
23 MWCNTs have already been reported by our group.<sup>29</sup> The polar surface of MWCNTs may  
24  
25 attract Ca<sup>2+</sup> ions, indicating a preferred interaction site on specific crystal surface faces during  
26  
27 the nucleation and crystal growth of CaOx in a manner similar to biomolecules in biogenic  
28  
29 minerals. Then, crystal habit is determined by the relative rates of growth of different crystal  
30  
31 faces, with the slow growing surfaces dominating the final form. It is believed that these faces  
32  
33 may be stabilised via stereoselective adsorption of the carboxylic acid groups via bidentate  
34  
35 carboxylate binding. Figure 3 shows the chrono-potentiometric measurements obtained during  
36  
37 the EC of CaOx using 0.03 mg/mL functionalized MWCNTs and by applying a 9-mA current in  
38  
39 a closed system at 37 °C or 60 °C for 5 min. This short amount of time has been reported by us  
40  
41 to be a sufficient amount of time to induce the formation of CaOx crystals via the EC assays.<sup>30</sup>  
42  
43  
44  
45  
46  
47  
48

### 49 **Figure 3.**

50  
51 It is seen that both citrate and the functionalized MCWNTs inhibit the formation of CaOx  
52  
53 crystals by EC at 37 °C and 60 °C, and MWCNT-IA is the most efficient inhibitor in both the EC  
54  
55  
56  
57  
58  
59  
60

1  
2  
3 systems. The order in which the functionalized MWCNTs templates inhibit crystal formation  
4 was found to be MWCNT-IA > MWCNT-MMI > MWCNT-MODI > citrate. The more  
5  
6 noticeable inhibition effect of MWCNT-IA was recorded at 60 °C. The higher temperature  
7  
8 allows for a more homogeneous suspension of the CNTs in the electrolytic solution, facilitating  
9  
10 the adsorption/inclusion of MWCNT-IA in the crystalline lattice. This is probably associated  
11  
12 with a better disentanglement of the functionalized MWCNTs.  
13  
14  
15

16  
17 The inhibition effect of citrate and all the MWCNTs templates during the EC of CaOx by  
18  
19 applying a 9-mA current in a closed system at 37 °C or 60 °C was compared with the control  
20  
21 experiment, although more CaOx crystals precipitated under these conditions (Figure S5). We  
22  
23 found that when the EC was performed at a higher temperature, the potential value increased for  
24  
25 each applied current at 37 °C and 60 °C. It was also found that the potentiometric response  
26  
27 curves begin to stabilize by increasing the temperature, and the effect of the system decreases the  
28  
29 variation between each point measured in the EC of CaOx. In addition, we have reported that  
30  
31 anionic MWCNTs also acted as efficient inhibitors in the *in vitro* CaCO<sub>3</sub> crystallization.<sup>31</sup>  
32  
33  
34  
35

36  
37 Herein, MWCNT-IA was a better inhibitor template than the well-known organic citrate,  
38  
39 which was used to inhibit the EC of CaOx at 37 °C and 60 °C. The morphology (Figure 4) and  
40  
41 hydrated crystal forms (Figure 5) of CaOx obtained via EC using citrate and all the MWCNTs by  
42  
43 applying a 9-mA current for 5 min in a closed system at 37 °C or 60 °C were analyzed by SEM  
44  
45 and XRD, respectively. Figure 4 shows the SEM images of representative CaOx crystals  
46  
47 obtained in the presence of all the functionalized MWCNTs and citrate via EC by applying a 9-  
48  
49 mA current at 37 °C. The SEM analysis of CaOx under the same experimental conditions but at  
50  
51 60 °C was also performed (Figure S6). In general, Figure 4 shows that when citrate was used as  
52  
53 the additive at 37 °C, few undifferentiated round CaOx crystals (4 μm) were obtained (Figure  
54  
55  
56  
57  
58  
59  
60

1  
2  
3 4A-B). When MWCNT-IA was used, abundant round COM crystals (5  $\mu\text{m}$ ) with porous surfaces  
4  
5 were found at 37  $^{\circ}\text{C}$  (Figure 4C-D). When MWCNT-MMI was used, scarce COD crystals (5  
6  
7  $\mu\text{m}$ ) and small undifferentiated pieces were observed at 37  $^{\circ}\text{C}$  (Figure 4E-F). Rough COM and  
8  
9 COD crystals (40  $\mu\text{m}$ ) were observed at 37  $^{\circ}\text{C}$  when MWCNT-MODI was utilized (Figure 4G-  
10  
11 H).  
12  
13

#### 14 15 **Figure 4.**

16  
17 The optical and SEM analyses of the CaOx crystals obtained when MWCNTs were used as  
18  
19 templates and by using the chrono-potentiometry method via EC are summarized in Table 2.  
20  
21  
22

#### 23 **Table 2.**

24  
25 In addition, an SEM-EDX analysis of the surface of the ITO substrates was also performed to  
26  
27 determine the elemental composition of the deposited CaOx crystals. In the absence of additives,  
28  
29 the chemical composition of CaOx did not differ from theoretical predictions. As is known, XRD  
30  
31 is a more suitable technique than SEM-EDX to identify inorganic constituents in KS by their  
32  
33 unique diffraction patterns, which allows the identification of unknown crystalline  
34  
35 substances.<sup>14,32-34</sup> Therefore, XRD was performed on the CaOx crystals formed on the surface of  
36  
37 the ITO substrates via the EC experiments by applying 3, 9, 15, and 18 mA currents at 37  $^{\circ}\text{C}$  and  
38  
39 60  $^{\circ}\text{C}$  (Figure S7). In general, the XRD patterns of the CaOx crystals electrodeposited on ITO  
40  
41 were quite similar to each other. Figure 5 (A-D) shows the XRD patterns of the CaOx crystals  
42  
43 grown in the presence of citrate and all the functionalized MWCNTs when a 9-mA current was  
44  
45 applied at both 37  $^{\circ}\text{C}$  and 60  $^{\circ}\text{C}$ . The XRD patterns showed diffraction peaks at  $2\theta = 15^{\circ}$ ,  $23.2^{\circ}$ ,  
46  
47  $24.2^{\circ}$ ,  $25.8^{\circ}$ ,  $30^{\circ}$ ,  $35^{\circ}$ ,  $50^{\circ}$  and  $53^{\circ}$ , confirming the coexistence of COD and COM crystals. It  
48  
49 was found that the intensities of the crystallographic peaks of COM and COD were small, and  
50  
51 both hydrates were promoted at these temperatures. Surprisingly, the diffraction peak  
52  
53  
54  
55  
56  
57  
58  
59  
60

1  
2  
3 corresponding to the (200) plane of COM at 15° did not appear when MWCNT-IA was utilized  
4  
5 as template at both temperatures.  
6  
7

### 8 **Figure 5.**

9  
10 The differences between the diffractograms of the CaOx crystals obtained using control  
11 samples and all the MWCNTs templates are also presented (Tables S2, S3, S4 and S5). The  
12 XRD analysis demonstrated that the sampled obtained using functionalized MWCNTs are  
13  
14 capable of modulating the nucleation and growth of CaOx crystals obtained via EC.<sup>30</sup>  
15  
16

17  
18 Prior EC studies on CaOx obtained by the cathodic reduction of acidic aqueous solutions  
19 containing calcium and oxalate ions have highlighted the importance of electrodeposition to the  
20  
21 polymorphic modification of CaOx crystals.<sup>15</sup> These authors found that the stabilization of the  
22  
23 COD was favored when an electric current density of 6 mA/cm<sup>2</sup> was applied at 23 °C, whereas  
24  
25 the formation of COM crystals was promoted when an electric current density of 3 and 6  
26  
27 mA/cm<sup>2</sup> were applied at 65 °C. Both hydrates showed oriented growth with respect to the  
28  
29 substrate under different deposition conditions. Therefore, COD is formed first, and then, it  
30  
31 transforms to COM in a manner similar to that occurs in nature, namely, by dissolution and  
32  
33 reprecipitation mechanisms. The COM crystals were stabilized at a pH of 11 and with an electric  
34  
35 current density of 6 mA/cm<sup>2</sup> applied at 65 °C. The current study demonstrated that when  
36  
37 functionalized MWCNTs are used as template via the EC of CaOx, the selective control of the  
38  
39 morphology and polymorphism of CaOx can be achieved, and thus, the deposition of COM and  
40  
41 COD crystals on ITO is promoted, which act as effective inhibitors of the pathological COM  
42  
43 polymorph. It is known that the inorganic mineral deposition occurs only in the immediacy of the  
44  
45 conducting ITO's surface and not in the bulk of electrolytic solution.<sup>15,30</sup> Therefore, the  
46  
47 mechanism of the modulation of CaOx during the EC process occurs by the adsorbed MWCNTs  
48  
49  
50  
51  
52  
53  
54  
55  
56  
57  
58  
59  
60

1  
2  
3 used as template onto ITO surface via electrostatic interaction (Figure 6 A-B). In general, Figure  
4 6 illustrates how carboxylic acid (COOH) groups of adsorbed MWCNT-IA onto ITO surface  
5 (Figure 6A) are more prone than ester groups of adsorbed MWCNTs functionalized either with  
6 MMI (Figure 6B) or MODI to form electrostatic interaction with  $\text{Ca}^{2+}$  ions. However, the  
7 presence of unreacted COOH groups on the surface of functionalized MWCNTs could also  
8 interact with  $\text{Ca}^{2+}$  ions. The aforementioned mechanism is backed by our experimental data,  
9 where the zeta potential presented negative values for functionalized MWCNTs at pH 4.0, in  
10 which the *in vitro* EC of CaOx occurs and positive values for pristine MWCNT.<sup>29</sup> In addition, we  
11 found that the concentration of unreacted –COOH groups, determined by an automated acid-base  
12 titration, are still present in the range of 12.0 - 15.0 mmol/g for these functionalized MWCNTs  
13 templates instead of *ca.* 1.8 mmol/g for the pristine MWCNTs.<sup>29</sup> Therefore, the crystal habit in  
14 both cases of functionalized MWCNTs template is the resulting of all electrostatic interactions  
15 determined by the relative rates of growth of different crystal faces, with the slow growing  
16 surfaces dominating the final form.  
17  
18  
19  
20  
21  
22  
23  
24  
25  
26  
27  
28  
29  
30  
31  
32  
33  
34  
35

### 36 **Figure 6.**

37  
38 Moreover, we believe that by varying the electrical current during chrono-potentiometry, it is  
39 possible to detect the precise moment when the ITO substrate is covered with CaOx crystals or to  
40 assess an electrochemical approach to determine when the transformation of COD to COM  
41 occurs. We found that the potentiometric response curves of the CaOx crystals obtained using a  
42 closed system for the *in vitro* EC showed a significant and constant increase in the potential  
43 values at both temperatures, which were maintained over time. The electrochemical approach for  
44 the deposition of inorganic minerals under laboratory conditions is relatively cheap, fast and  
45 simple.<sup>35</sup> We identified the experimental conditions necessary to carry out the *in vitro* EC of  
46  
47  
48  
49  
50  
51  
52  
53  
54  
55  
56  
57  
58  
59  
60

1  
2  
3 CaOx to evaluate the effect of different functionalized MWCNTs, which can also be used to  
4 generate natural or synthetic molecules and nanomaterials. The formation of CaOx crystals was  
5 reproducible, as shown by the statistical analysis (Figures S8, S9 and S10). In this regard, the  
6 GLM model was adjusted according to its theoretical quantiles (Figure S8), treatments (Figure  
7 S9) and temperatures (Figure S10). We used citrate as the positive control in the EC of CaOx,  
8 because this molecule is widely used in the symptomatic treatment of human and mammalian  
9 urolithiasis.<sup>12,36</sup> The applied statistical model allowed for the prediction of the data analysis in an  
10 optimum manner. The tests of the marginal hypotheses indicated that there were treatment and  
11 temperature effects. The Bonferroni correction was used due to the large amount of data (Table  
12 S6). The treatment effect between citrate and the rest of the treatments showed that MWCNT-IA  
13 has a lower average (Table S7) and that there was a temperature effect on the means of the  
14 treatments, which were all more efficient at a higher temperature (Table S8). These values are  
15 similar to each other for treatments at 37 °C and 60 °C but are different than the control, and  
16 thus, this was deemed to be an appropriate comparison with the functionalized MWCNTs.<sup>11,36</sup>  
17 The EDX results obtained via EC were similar to those reported by Kumar et al.<sup>32</sup> and Didenko  
18 et al.<sup>37</sup> The XRD patterns of CaOx allowed us to compare the obtained diffractograms with those  
19 known in the literature.<sup>11,35-37</sup> A mixed crystalline XRD pattern was identified, where COM  
20 corresponded to the predominant crystallographic peaks, but COD was also found.

21  
22  
23  
24  
25  
26  
27  
28  
29  
30  
31  
32  
33  
34  
35  
36  
37  
38  
39  
40  
41  
42  
43  
44  
45 Our results indicate that the functionalized MWCNTs induce morphological changes of CaOx  
46 and could control the polymorphism of CaOx by the direct interaction of MWCNTs containing  
47 carboxylic or ester groups with specific facets of CaOx crystals in a manner similar to how  
48 urinary proteins induce effects on CaOx.<sup>38</sup> Citrate and MWCNT-IA, which are both anionic  
49 compounds, can bind Ca<sup>2+</sup> ions during the EC of CaOx in a better way than MWCNT-MMI and  
50  
51  
52  
53  
54  
55  
56  
57  
58  
59  
60

1  
2  
3 MWCNT-MODI. This is why it is very important to analyze the electrochemical solution to  
4  
5 determine the amount of  $\text{Ca}^{2+}$  in solution and to understand how urinary molecules prevent the  
6  
7 formation of KS.<sup>39</sup> We state that the experimental conditions are indicators of the modulation of  
8  
9 the EC of CaOx. MWCNTs induces changes in the morphology and acted in an active way to  
10  
11 control the nucleation and growth of CaOx crystals. In fact, MWCNT-IA inhibits the (200) plane  
12  
13 of COM, which corresponds to the peak at  $15^\circ$  in the XRD pattern, in a similar manner as  
14  
15 biomolecules behave in mammalian calculi. Oxalate ions may attract  $\text{Ca}^{2+}$  ions, causing CaOx  
16  
17 crystals to form; however, if the  $\text{Ca}^{2+}$  ions are not available in the electrolytic solution due to  
18  
19 their interactions with MWCNTs, the  $\text{Ca}^{2+}$  ions may not bind oxalate. Carboxylic acid groups are  
20  
21 better than ester groups for binding  $\text{Ca}^{2+}$  ions and thus inhibit nucleation and control the growth  
22  
23 of CaOx crystals.<sup>40</sup>  
24  
25  
26  
27  
28  
29  
30

#### 31 4. CONCLUSIONS

32  
33 The ability of MWCNTs functionalized with itaconic acid (IA) and IA esters (MMI and MODI),  
34  
35 which are used as template, on the nucleation, growth and the formation of different CaOx  
36  
37 hydrate crystals via *in vitro* EC by applying a 9-mA current at 37 °C and 60 °C for 5 min was  
38  
39 demonstrated. The order in which the templates inhibit the formation of different hydrate forms  
40  
41 of CaOx was found to be MWCNT-IA > MWCNT-MMI > MWCNT-MODI > citrate. The  
42  
43 mechanism of the modulation of CaOx during the EC can be explained by the adsorbed  
44  
45 MWCNTs template on ITO glass substrate. It was found that the electrostatic interaction of  
46  
47 COOH groups of IA moieties in MWCNT-IA would be better  $\text{Ca}^{2+}$  ions-binding sites than IA  
48  
49 ester groups in MWCNT-MMI and MWCNT-MODI. In addition, types and morphologies of  
50  
51  
52  
53  
54  
55  
56  
57  
58  
59  
60



1  
2  
3 CaOx crystals including the COM and COD hydrates was stabilized by the EC of CaOx applying  
4 a 9-mA current at 37 °C and 60 °C for 5 min.  
5  
6  
7

## 8 **ASSOCIATED CONTENT**

### 9 **Supporting Information.**

10  
11  
12 Detailed synthesis and experimental procedure. Figures S1-10 and Tables S1-9. Electronic  
13  
14  
15 Supplementary Information (ESI) available: The experimental procedures for the  
16  
17  
18 functionalization of MWCNTs, the EC of CaOx, the statistical strategy used to study the  
19  
20  
21 electrochemical response obtained by EC, the spectroscopic, optical, and SEM-EDX analyses of  
22  
23  
24 CaOx and the TEM analyses of the MWCNTs are given in the Supporting Information.  
25  
26  
27

## 28 **AUTHOR INFORMATION**

### 29 **Corresponding Author.**

30  
31 \*E-mail: [aneira@uchile.cl](mailto:aneira@uchile.cl). Fax: +56-2-29785526. Tel: +56-2-29785674.  
32  
33  
34  
35

### 36 **Author Contributions**

37  
38  
39 The manuscript was written using contributions of all the authors. All the authors have approved  
40  
41  
42 the final version of this manuscript.  
43  
44

### 45 **ORCID:**

46  
47  
48 Andrónico Neira-Carrillo: 0000-0003-0060-7518  
49  
50

### 51 **Notes**

52  
53 The authors declare no competing financial interest.  
54  
55  
56  
57  
58  
59  
60

## ACKNOWLEDGMENT

The authors acknowledge the financial support of the Chilean Council for Science and Technology (CONICYT) (Fondecyt 1171520 & 1140660) and Fondap ACCDiS 15130011.

## ABBREVIATIONS

EC, electrocrystallization; CaOx, calcium oxalate; CNT, carbon nanotube; MWCNT, multiwalled CNT; IA, itaconic acid; MMI, monomethyl itaconate; MODI, monoctadecyl itaconate; COM, CaOx monohydrate; COD, CaOx dihydrate; KS, kidney stones; ITO, indium tin oxide.

## REFERENCES

- (1) Mann, S. *Biom mineralization Principles and Concepts in Bioinorganic Materials Chemistry*, Oxford University Press: Oxford, 2001.
- (2) Borissova, A.; Goltz, G.; Kavanagh, J.; Wilkins, T. Reverse Engineering the kidney: Modeling Calcium Oxalate Monohydrate Crystallization in the Nephron. *Med. Biol. Eng. Comput.* **2010**, 48, 649-659.
- (3) Wesson, J. A.; Ward, M. D. Pathological Biom mineralization of Kidney Stone. *Elements* **2007**, 3, 415-421.
- (4) Neira-Carrillo, A.; Vásquez-Quitral, P. Formación de Cálculos Renales de Oxalato Cálculo en Mamíferos. *Av. Cs. Vet.* **2010**, 25, 41-52.

- 1  
2  
3 (5) Long, L. O.; Park, S. Update on Nephrolithiasis Management. *Minerva Urol. Nefrol.*  
4 **2007**, 59, 317-325.  
5  
6  
7  
8  
9 (6) Aitipamula, S.; Nangia, A. Polymorphism: Fundamentals and Applications. *In*  
10 *Supramolecular Chemistry: From Molecules to Nanomaterials*; Steed, J. W., Gale, P. A.,  
11 Eds.; John Wiley & Sons, 2012; pp 2957-2974.  
12  
13  
14  
15  
16 (7) Nangia, A. Nomenclature in crystal engineering. *In Encyclopedia of Supramolecular*  
17 *Chemistry*; Atwood, J. L.; Steed, J. W., Eds.; Marcel Dekker: New York, 2004; Vol. 2, pp  
18 967-972.  
19  
20  
21  
22  
23  
24 (8) Monje, P. M.; Baran E. Characterization of Calcium Oxalates Generated as Biominerals  
25 in Cacti. *J. Plant Physiol.* **2002**, 128, 707-713.  
26  
27  
28  
29  
30 (9) Wesson, J. A.; Worcester, E. M.; Wiessner, J. H.; Mandel, N. S.; Keinman, J. G. Control  
31 of Calcium Oxalate Crystal Structure and Cell Adherence by Urinary Macromolecules.  
32 *Kidney Int.* **1998**, 53, 952-957.  
33  
34  
35  
36  
37  
38 (10) Finlayson, B. Physicochemical Aspects of Urolithiasis. *Kidney Int.* **1978**, 13, 344-360.  
39  
40  
41 (11) Zhang, D.; Qi, L; Ma, J.; Cheng, H. Morphological Control of Calcium Oxalate  
42 Dihydrate by a Double-Hydrophilic Block Copolymer. *Chem. Mater.* **2002**, 14, 2450-  
43 2457.  
44  
45  
46  
47  
48  
49 (12) Kato, Y.; Yamaguchi, S.; Yachiku, S.; Nakazono, S.; Hori, J.; Wada, N.; Hou, K.  
50 Changes in Urinary Parameters after Oral Administration of Potassium-Sodium Citrate  
51 and Magnesium Oxide to Prevent Urolithiasis. *Urol.* **2004**, 63, 7-12.  
52  
53  
54  
55  
56  
57  
58  
59  
60

- 1  
2  
3 (13) Joseph, S.; Kamath, P. V. Electrochemical Deposition of Cu<sub>2</sub>O on Stainless Steel  
4 Substrates: Promotion and Suppression of Oriented Crystallization. *Solid State Sci.* **2008**,  
5 10, 1215-1221.  
6  
7  
8  
9  
10  
11 (14) Saha, S.; Sultana, S.; Islam, M. M.; Rahman, M. M.; Mollah, M. Y. A.; Susan, M. A. B.  
12 H. Electrodeposition of Cobalt with Tunable Morphology From Reverse Micellar  
13 Solution. *Ionics* **2014**, 20, 1175-1181.  
14  
15  
16  
17  
18  
19 (15) Joseph, J.; Kamath, P. V. J. Synthesis of Different Polymorphic Modifications of  
20 Calcium Oxalate by Electrodeposition. *Solid State Electr.* **2009**, 14, 1481-1486.  
21  
22  
23  
24 (16) Gebauer, D.; Völkel, A.; Cölfen, H. Stable Prenucleation Calcium Carbonate Clusters.  
25 *Science* **2008**, 322, 1819-1822.  
26  
27  
28  
29  
30 (17) Dinamani, M.; Kamath, P. V.; Seshadri, R. Deposition of Oriented SrSO<sub>4</sub> Coatings by  
31 Electrogeneration of Acid. *Solid State Sci.* **2003**, 5, 805-810.  
32  
33  
34  
35  
36 (18) Zhao, L.; Gao, L. Novel in Situ Synthesis of MWNTs-Hydroxyapatite Composites.  
37 *Carbon* **2004**, 42, 423-426.  
38  
39  
40  
41 (19) Zhao, B.; Hu, H.; Mandal, S.; Haddon, R. A. Bone Mimic Based on the Self-Assembly of  
42 Hydroxyapatite on Chemically Functionalized Single-Walled Carbon Nanotubes. *Chem.*  
43 *Mater.* **2005**, 17, 3235-3241.  
44  
45  
46  
47  
48  
49 (20) Govindaraj, D.; Rajan, M.; Munusamy, M. A.; Alarfaj, A. A.; Higuchi, A.; Kumar, S. S.  
50 Carbon Nanotubes/Pectin/Minerals Substituted Apatite Nanocomposite Depositions on  
51  
52  
53  
54  
55  
56  
57  
58  
59  
60

- 1  
2  
3 Anodized Titanium for Hand Tissue Implant: *In Vivo* Biological Performance. *Mater.*  
4  
5 *Chem. Phys.* **2017**, 194, 77-89.  
6  
7  
8  
9 (21) Rieger, J.; M. Kellermeier, M.; Nicoleau, L. Formation of Nanoparticles and  
10 Nanostructures - An Industrial Perspective on CaCO<sub>3</sub>, Cement, and Polymers. *Angew.*  
11 *Chem. Int. Ed.* **2014**, 53, 12380-12396.  
12  
13  
14  
15 (22) Anderson, R. E.; Barron, A. R. Barron. Effect of Carbon Nanomaterials on Calcium  
16 Carbonate Crystallization. *Main Group Chem.* **2005**, 4, 279-289.  
17  
18  
19  
20 (23) Wesson, J. A.; Ganne, V.; Beshensky, A. M.; Keinman, J. G. Kleinman. Regulation by  
21 Macromolecules of Calcium Oxalate Crystal Aggregation in Stone Formers. *Urol. Res.*  
22 **2005**, 33, 206-212.  
23  
24  
25  
26  
27 (24) Saha, S.; Verma, R. J. Inhibition of Calcium Oxalate Crystallisation In Vitro by An  
28 Extract of *Bergenia Ciliata*. *Arab. J. Urol.* **2013**, 11, 187-192.  
29  
30  
31  
32 (25) Tasis, D.; Tagmatarchis, N.; Bianco, A.; Prato, M. Chemistry of Carbon Nanotubes.  
33 *Chem. Rev.* **2006**, 106, 1105-1136.  
34  
35  
36  
37 (26) Shin, U. S.; Yoon, I. K.; Lee, G. S.; Jang, W. C. Knowles, J. C.; Kim, H. W. Carbon  
38 Nanotubes in Nanocomposites and Hybrids with Hydroxyapatite for Bone Replacements.  
39 *J. Tissue Eng.* **2011**, 2011, 674287.  
40  
41  
42  
43 (27) Gomez, V.; Correasa C.; Barron, A. R. Effect of Carbon Nanotubes on Calcium  
44 Carbonate/Calcium Silicate Phase and Morphology. *Main Group Chem.* **2017**, 16, 57-65.  
45  
46  
47  
48  
49 (28) Tasis, D.; Pispas, S.; Galiotis, C.; Bouropoulos, N. Growth of Calcium Carbonate on  
50 Non-Covalently Modified Carbon Nanotubes. *Mater. Lett.* **2007**, 61, 5044-5046.  
51  
52  
53  
54  
55  
56  
57  
58  
59  
60

- 1  
2  
3 (29) Neira-Carrillo, A.; Vásquez-Quitral, P.; Sánchez, M.; Farhadi-Khouzani, M.; Aguilar-  
4 Bolados, H.; Yazdani-Pedram, M.; Cölfen, H. Functionalized Multiwalled CNTs in  
5 Classical and Nonclassical CaCO<sub>3</sub> Crystallization. *Nanomaterials* **2019**, 9(8), 1169.  
6 DOI:10.3390/nano9081169.  
7  
8  
9  
10  
11  
12 (30) Neira-Carrillo, A.; Vásquez-Quitral, P.; Sánchez, M.; Vargas-Fernández, A.; Silva, J. F.  
13 Control of Calcium Oxalate Morphology Through Electrocrystallization as an  
14 Electrochemical Approach for Preventing Pathological Disease. *Ionics* **2015**, 21, 3141-  
15 3149.  
16  
17  
18  
19  
20  
21  
22 (31) Sánchez, M.; Vásquez-Quitral, P.; Butto, N.; Díaz-Soler, F.; Yazdani-Pedram, M.; Silva,  
23 J. F.; Neira-Carrillo, A. Effect of Alginate from Chilean *Lessonia nigrescens* and  
24 MWCNTs on CaCO<sub>3</sub> Crystallization by Classical and Non-Classical Methods. *Crystals*  
25 **2018**, 8, 1-15.  
26  
27  
28  
29  
30  
31  
32 (32) Kumar, N.; Singh, P.; Kumar, S. Physical, X-ray Diffraction and Scanning Electron  
33 Microscopic Studies of Uroliths. *Indian J. Biochem. & Biophys.* **2006**, 43, 226-232.  
34  
35  
36  
37  
38 (33) Neira-Carrillo, A.; Vásquez-Quitral, P.; Fernández, M. S.; Luengo-Ponce, F.; Yazdani-  
39 Pedram, M.; Cölfen, H.; Arias, J. L. Preparation of Sulfonated Polymethylsiloxane as  
40 Additive for the Selective Calcium Oxalate Crystallization. *Eur. J. Inorg. Chem.* **2015**, 7,  
41 1167-1177.  
42  
43  
44  
45  
46  
47  
48 (34) Kirboga, S.; Öner, M. Inhibition of Calcium Oxalate Crystallization by graft copolymers.  
49 *Cryst. Growth and Des.* **2009**, 9, 2159-2167.  
50  
51  
52  
53  
54  
55  
56  
57  
58  
59  
60

- 1  
2  
3 (35) Aoki, Y.; Huang, J.; Kunitake, T. Electro-Conductive Nanotubular Sheet of Indium Tin  
4 Oxide as Fabricated from the Cellulose Template. *J. Mater. Chem.* **2009**, 16, 292-297.  
5  
6  
7  
8 (36) Curhan, G. C. Epidemiology of Stone Disease. *Urol. Clin. North. Am.* **2007**, 34, 287-293.  
9  
10  
11 (37) Didenko, L.; Tolordava, E.; Perpanova, T.; Shevlyagina, T.; Boravaya, Y.; Romanova,  
12 Y.; Cazzaniga, M.; Curia, R.; Milani, R.; Savoia, C.; Tatti, F. Electron Microscopy  
13 Investigation of Urine Stones Suggests How to Prevent Post-Operation Septic  
14 Complications in Nephrolithiasis. *J. Applied Med. Sci.* **2004**, 3, 19-34.  
15  
16  
17 (38) Addadi, L.; Weiner, S. Interactions Between Acidic Proteins and Crystals:  
18 Stereochemical Requirements in Biomineralization. *Proc. Natl. Acad. Sci.* **1985**, 82,  
19 4110-4114.  
20  
21  
22 (39) Laube, N.; Klein, F.; Bernsmann, F. Kinetics of Calcium Oxalate Crystal Formation in  
23 Urine. *Urol.* **2017**, 45, 151-157.  
24  
25  
26 (40) Rieger, J.; Thieme, J.; Schmidt, C. Study of Precipitation Reactions by X-ray  
27 Microscopy: CaCO<sub>3</sub> Precipitation and the Effect of Polycarboxylates. *Langmuir* **2000**,  
28 16, 8300-8305.  
29  
30  
31  
32  
33  
34  
35  
36  
37  
38  
39  
40  
41  
42  
43  
44  
45  
46  
47  
48  
49  
50  
51  
52  
53  
54  
55  
56  
57  
58  
59  
60

**FIGURE CAPTIONS**

**Figure 1.** The experimental setup and procedure used to study the EC of CaOx.

**Figure 2.** Chrono-potentiometric measurements obtained during the EC of CaOx in (A) an open system and (B) a closed system by applying a 9-mA current for 5 min at 37 °C or 60 °C.

**Figure 3.** Chrono-potentiometric measurements obtained during the EC of CaOx with 0.03 mg/mL functionalized MWCNTs and by applying a 9-mA current in the closed system for 5 min at (A) 37 °C and (B) 60 °C.

**Figure 4.** SEM of the CaOx crystals obtained via EC by applying a 9-mA current at 37 °C with (A,B) citrate, (C,D) MWCNT-IA, (E,F) MWCNT-MMI and (G,H) MWCNT-MODI.

**Figure 5.** XRD patterns of the CaOx crystals obtained via EC and grown in the presence of (A) citrate, (B) MWCNT-IA, (C) MWCNT-MMI and (D) MWCNT-MODI on ITO substrates with a 9-mA current applied at 37 °C and 60 °C. The COM and COD crystals are marked with the letters M and D, respectively.

**Figure 6.** Schematic representation of electrostatic interaction between adsorbed MWCNTs used as template onto ITO surface and CaOx during EC. (A) MWCNT-IA and (B) MWCNT-MMI.



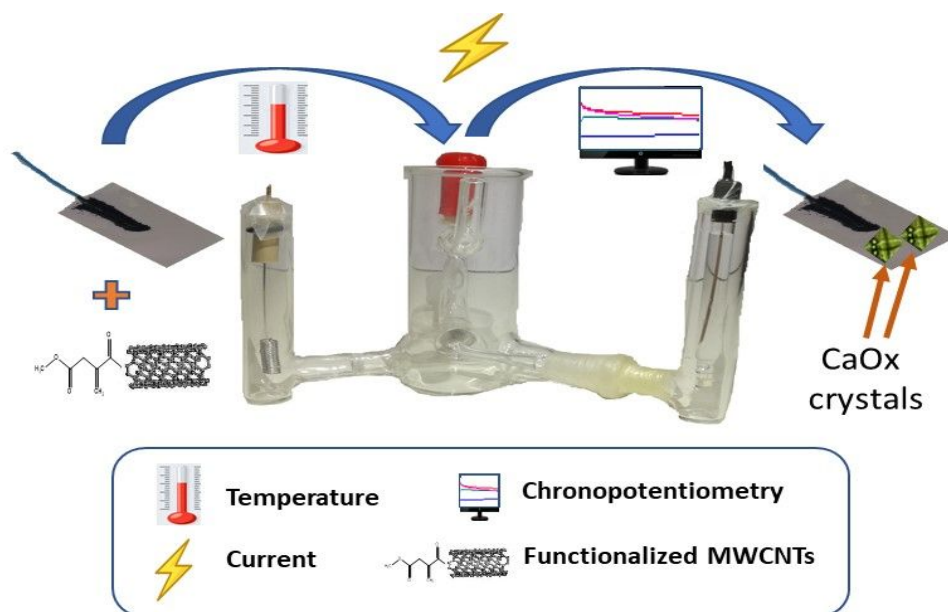


**Figure 1.** The experimental setup and procedure used to study the EC of CaOx.

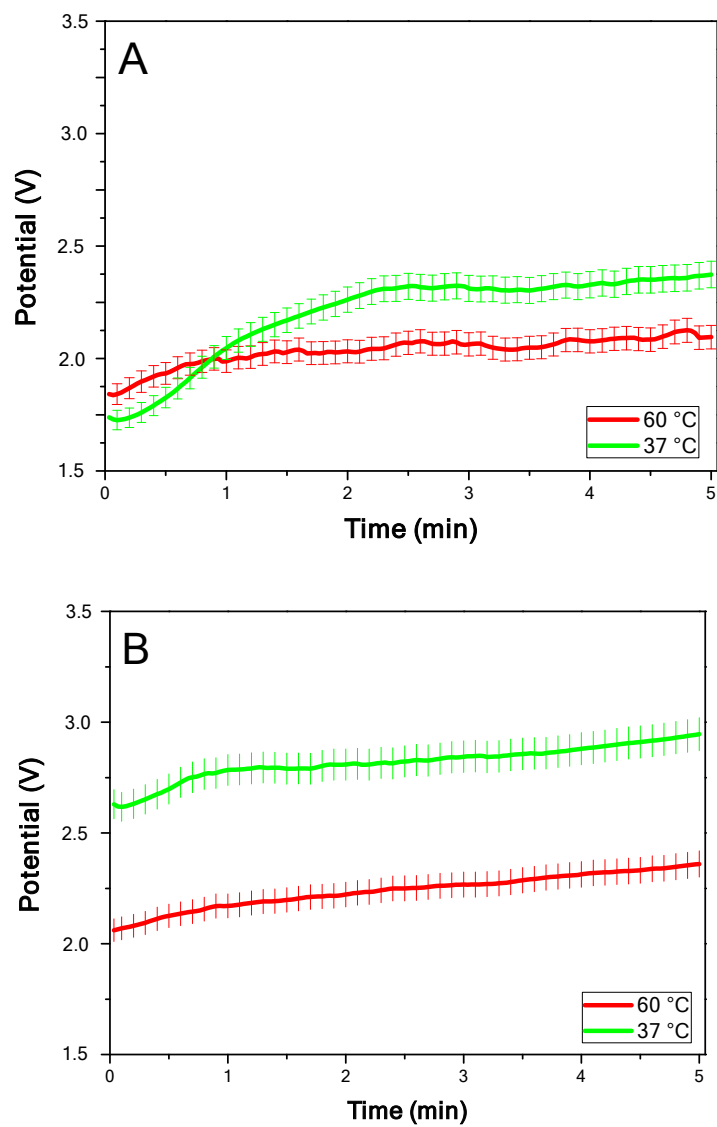


**Figure 2.** Chrono-potentiometric measurements obtained during the EC of CaOx in (A) an open system and (B) a closed system by applying a 9-mA current for 5 min at 37 °C or 60 °C.

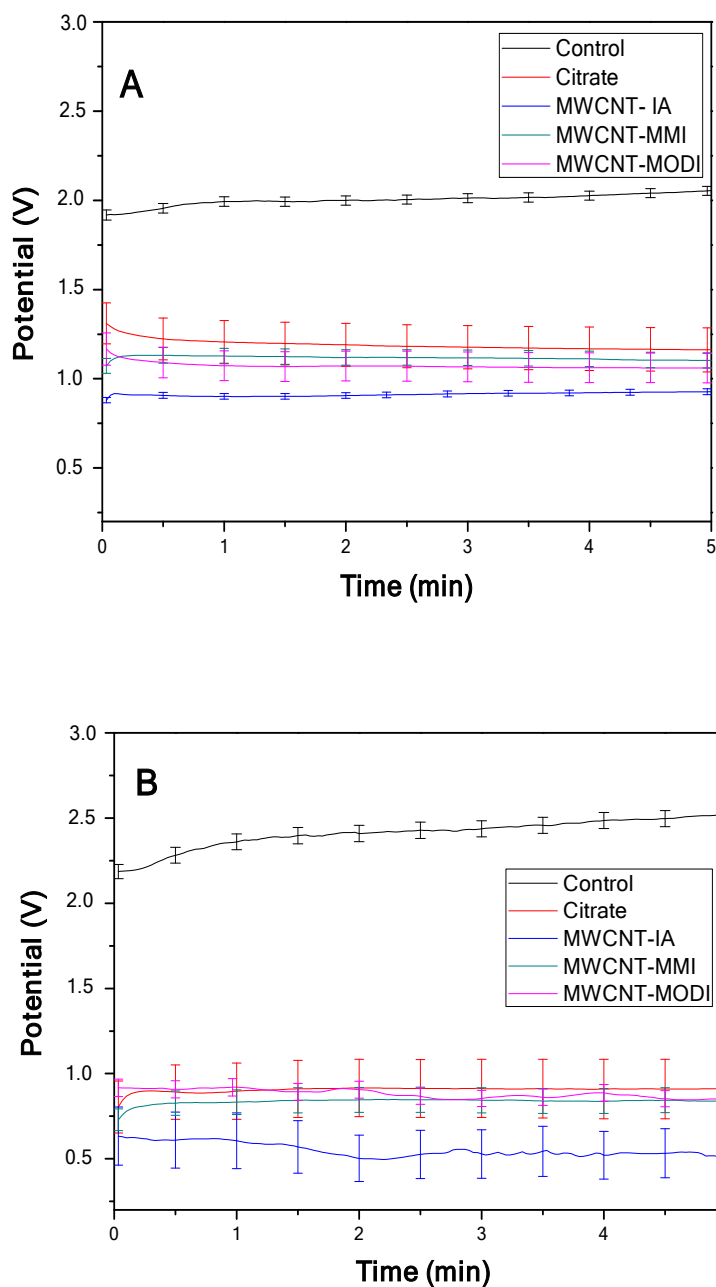


**Figure 3.** Chrono-potentiometric measurements obtained during the EC of CaOx with 0.03 mg/mL functionalized MWCNTs and by applying a 9-mA current in the closed system for 5 min at (A) 37 °C and (B) 60 °C.

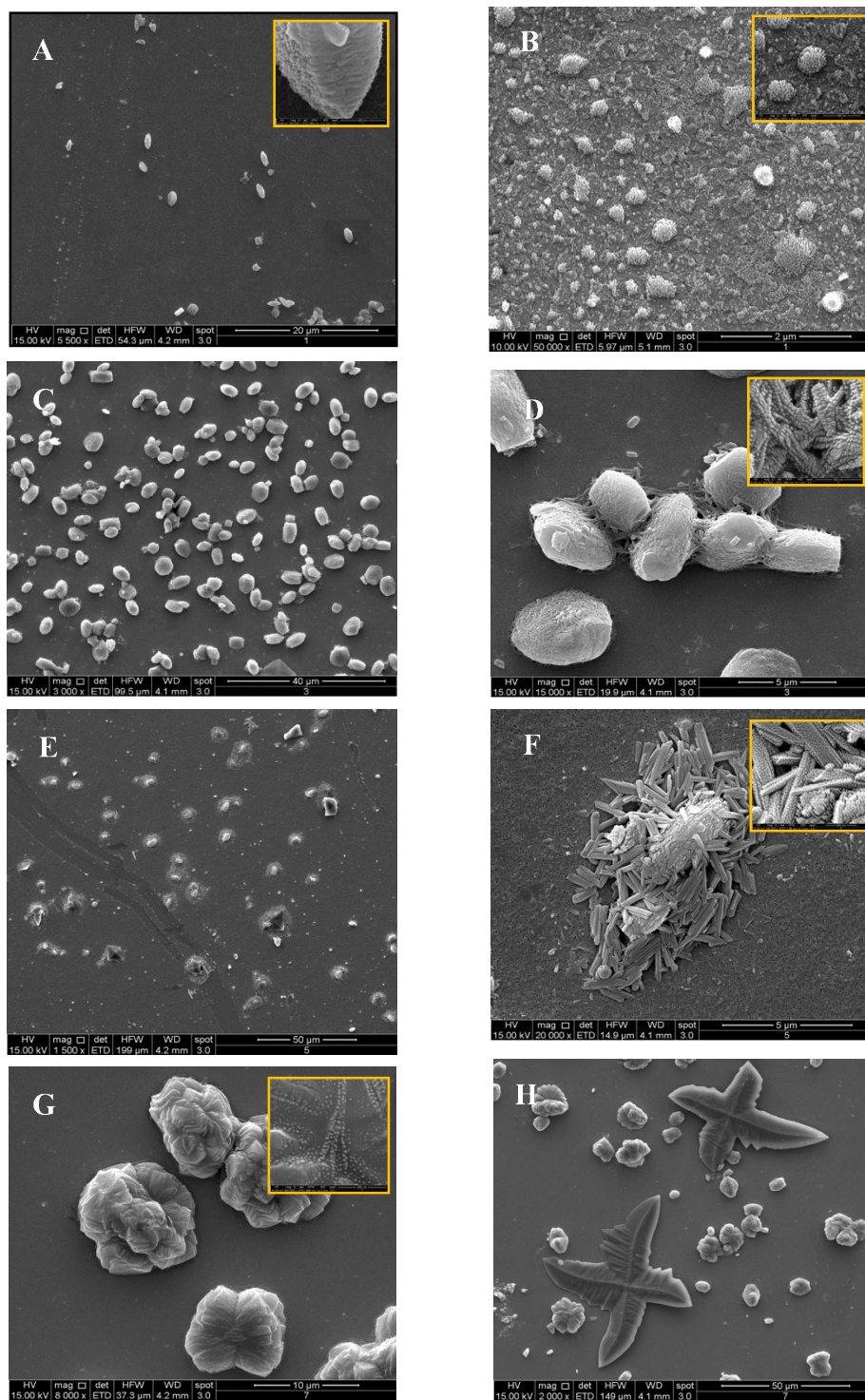


**Figure 4.** SEM of the CaOx crystals obtained via EC by applying a 9-mA current at 37 °C with (A,B) citrate, (C,D) MWCNT-IA, (E,F) MWCNT-MMI and (G,H) MWCNT-MODI.

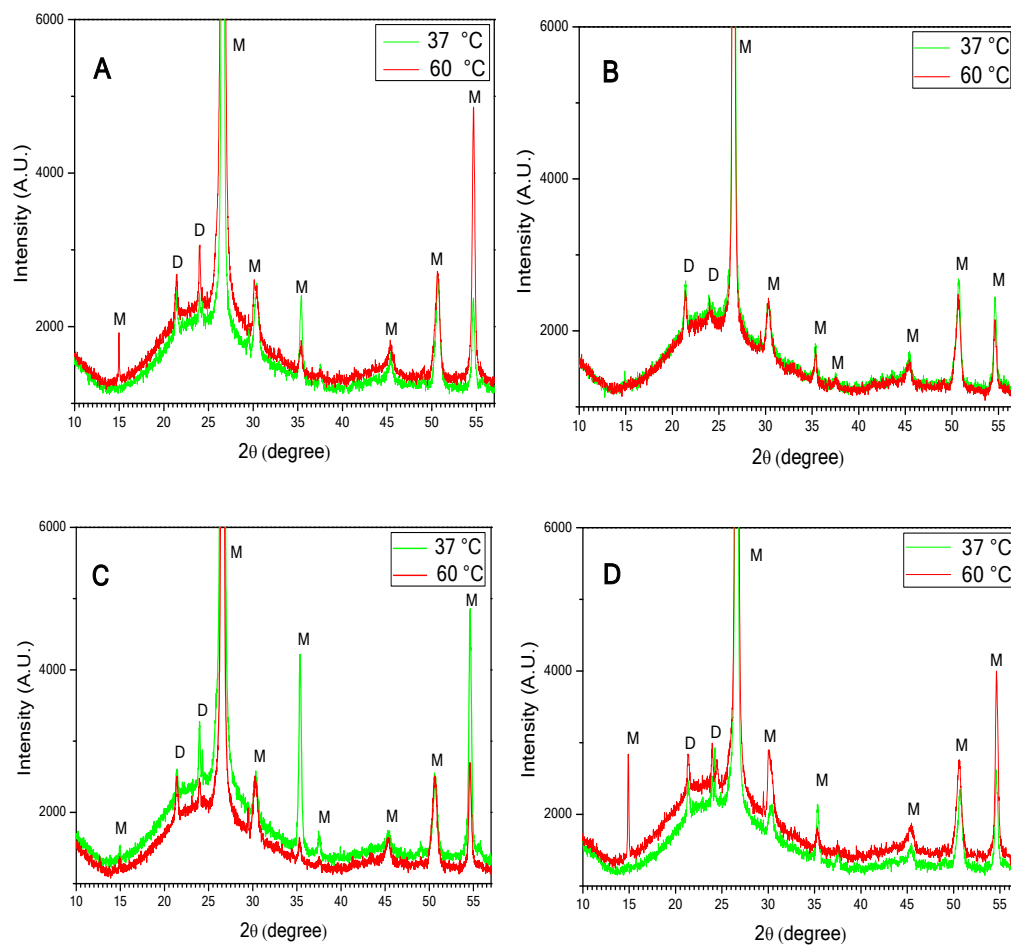


**Figure 5.** XRD patterns of the CaOx crystals obtained via EC and grown in the presence of (A) citrate, (B) MWCNT-IA, (C) MWCNT-MMI and (D) MWCNT-MODI on ITO substrates with a 9-mA current applied at 37 °C and 60 °C. The COM and COD crystals are marked with the letters M and D, respectively.

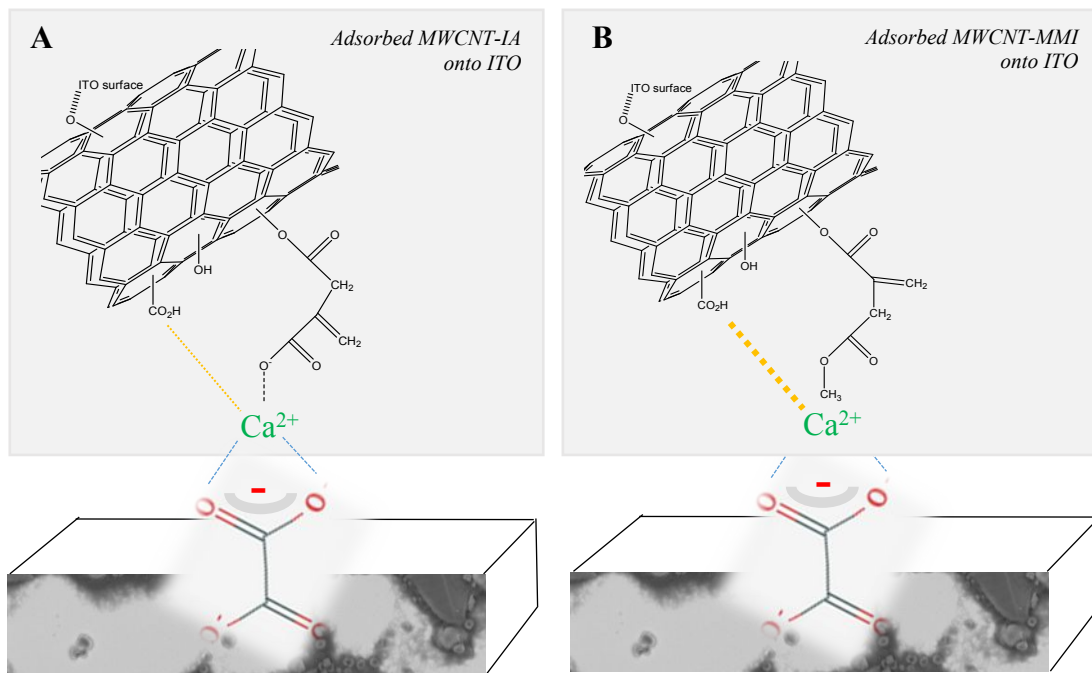


**Figure 6.** Schematic representation of electrostatic interaction between adsorbed MWCNTs used as template onto ITO surface and CaOx during EC. (A) MWCNT-IA and (B) MWCNT-MMI.

**TABLE CAPTIONS**

**Table 1.** Optical and scanning electron analyses of the CaOx crystals obtained in the absence of templates via EC by using the chrono-potentiometry method.

**Table 2.** Optical and scanning electron analyses of the CaOx crystals obtained in the presence of templates via EC by using the chrono-potentiometry method.

**Table 1.** Optical and scanning electron analyses of the CaO<sub>x</sub> crystals obtained in the absence of templates via EC by using the chrono-potentiometry method.

| <b>System</b> | <b>Current<br/>(mA)</b> | <b>Temperature<br/>(°C)</b> | <b>Main features</b>            |
|---------------|-------------------------|-----------------------------|---------------------------------|
| Closed        | 1                       | 37                          | Abundant crystals               |
| Open          | 1                       | 60                          | Large crystals, 120 μm          |
| Closed        | 1                       | 37                          | Abundant crystals               |
| Open          | 3                       | 60                          | Aggregated COD crystals         |
| Closed        | 3                       | 60                          | Typical COM crystals            |
| Open          | 6                       | 60                          | Large crystals, 100 μm          |
| Closed        | 6                       | 60                          | Aggregated typical COM crystals |
| Open          | 9                       | 60                          | Large crystals of COD, 60 μm    |
| Closed        | 9                       | 60                          | Aggregated crystals.            |
| Open          | 12                      | 60                          | Large crystals, 80 μm           |
| Closed        | 12                      | 60                          | Aggregated crystals             |
| Open          | 15                      | 60                          | Large crystals, 60 μm           |
| Closed        | 15                      | 60                          | Aggregated COD crystals         |
| Open          | 18                      | 37                          | Filamentous crystals            |
| Closed        | 18                      | 37                          | Aggregated crystals             |
| Open          | 21                      | 37                          | Aggregated crystals             |
| Closed        | 21                      | 60                          | Abundant aggregated crystals    |
| Open          | 24                      | 60                          | Crystals with undefined shapes  |

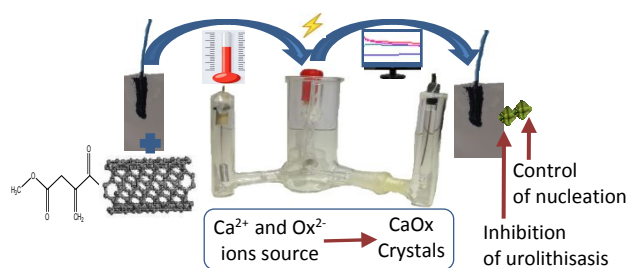


**Table 2.** Optical and scanning electron analyses of the CaOx crystals obtained in the presence of templates via EC by using the chrono-potentiometry method.

| Templates  | Current (mA) | Temperature (°C) | Main features   |
|------------|--------------|------------------|---|
| Control    | 9            | 37               | Undifferentiated small crystals   |
| Control    | 9            | 60               | Abundant and small COM crystals, 4 $\mu\text{m}$                                |
| Citrate    | 9            | 37               | Few round crystals, 4 $\mu\text{m}$ . Additionally, COD and COM crystals        |
| Citrate    | 9            | 60               | Abundant COM, 4 $\mu\text{m}$ , and COD, 10 $\mu\text{m}$ crystals              |
| MWCNT-IA   | 9            | 37               | Abundant round porous COM crystals, 5 $\mu\text{m}$                             |
| MWCNT-IA   | 9            | 60               | Abundant COD and COM crystals   |
| MWCNT-MMI  | 9            | 37               | Few COD crystals, 5 $\mu\text{m}$ and COM crystals with undifferentiated shapes |
| MWCNT-MMI  | 9            | 60               | Agglomerated of COD and COM crystals, 40 $\mu\text{m}$                          |
| MWCNT-MODI | 9            | 37               | COD crystals, 40 $\mu\text{m}$ , and rough COM crystals                         |
| MWCNT-MODI | 9            | 60               | Abundant COD crystals, 4 $\mu\text{m}$ and COM crystals, 2 $\mu\text{m}$        |

1  
2  
3  
4  
5  
6  
7  
8  
9  
10  
11 ***Effect of functionalized multiwalled CNTs on the***  
12  
13  
14  
15 ***selective formation of calcium oxalate crystals by***  
16  
17  
18  
19 ***electrocrystallization***  
20  
21  
22  
23

24 *Andrés Vargas-Fernández, † Marianela Sánchez, † Felipe Díaz-Soler, † Patricio Vásquez-*  
25 *Quitral, ‡ Mehrdad Yazdani-Pedram, § and Andrónico Neira-Carrillo \*†*  
26  
27  
28  
29  
30  
31  
32  
33  
34



46  
47 We report the use of inhibitor templates of CaOx crystallization that are more efficient than  
48 citrate by using multiwalled CNTs functionalized with itaconic acid and itaconic acid esters via  
49 an EC technique at 37 °C and 60 °C.  
50  
51  
52  
53  
54  
55  
56  
57  
58  
59  
60